Root Exudates Metabolic Profiling Suggests Distinct Defense Mechanisms Between Resistant and Susceptible Konjac Species against Soft Rot Disease

Jinping Wu
Jie Zhou
384881257@qq.com

Chaozhu Yang
Yidi Kuang
Chuangdong Qi
Fengling Guo
Qinghua Zhao

Research Article

Keywords: Amorphophallus konjac, disease resistance, defense mechanisms, root exudates

Posted Date: May 11th, 2024

DOI: https://doi.org/10.21203/rs.3.rs-4346041/v1

Abstract

In order to understand the relationship between the changes of konjac root exudates induced by soft rot disease, the differences of root exudates between resistant cultivars (*Amorphophallus bulbifer*, HB) and susceptible cultivars (*Amorphophallus konjac K.Koch*, HK) were analyzed by high-performance liquid chromatography tandem mass Fourier transform (UHPLC-q Exactive HF-X). The results showed that the 364 potential metabolites with significant differential amounts. Further analysis of the differential metabolites showed that there were 7 unique metabolites in HB, and 4 unique metabolites in HK. The fold change is 0.6143 and 0.5606 in HK/HB for 3-Fucosyllactose and buddleoflavonoloside, respectively. This showed that some sugars and flavonoids help improve the resistance of konjac soft rot. The analysis of metabolic pathways using the KEGG database revealed that the concentration of jasmonic acid (JA) in HB was significantly higher than in HK. JA metabolism was involved in regulating konjac soft rot disease resistance.

1. Introduction

China is the world's largest konjac production countries, accounting for 60% of the world's total output. With the development of konjac from sporadic cultivation to large-scale cultivation, the disease becomes more and more serious (Jiang et al. 2021).

The soft rot of konjac is one of the most serious diseases, which usually leads to yield loss of 30%-50%, sometimes more than 80% severe or results in the lack of harvest (Gu et al. 2018). The disease has become the main obstacle to the healthy development of konjac industry. At present, the control measures of konjac soft rot mainly include chemical control, intercropping and rotation. However, chemical control of konjac soft rot caused by pesticide residues, pollution and resistance, and it was difficult to carry out crop rotation and intercropping because of the limitation of land resources, so there were few effective measures to control konjac soft rot. Disease-resistant varieties are the most effective way to solve the soft rot disease, but the disease-resistant mechanism of konjac varieties is still unclear. It is very important to understand the resistance mechanism of resistant varieties to control soft rot disease. As a bacterial soil-borne disease, soft rot is closely related to root exudates in soil. Previous studies have shown that when plant roots are infected by pathogens, increased synthesis of root secondary metabolites can protect against the invasion of pathogens (Zhou et al. 2011). Root exudates are the most important secondary metabolites of plant roots, which can exert beneficial or harmful effects on soil microorganisms (including pathogens) and plants, and are closely related to plant disease resistance (Yang et al. 2014).

The *Amorphophallus konjac* (Araceae) genus contains more than 170 species, mainly distributed throughout Asia and Africa. Twenty-six species have been found in Sichuan, Chongqing, Yunan, Guizhou and Hubei Provinces in China (Liu et al. 2019). The resistance of different konjac species is different. *Amorphophallus konjac* K.Koch (HK) was susceptible cultivars (S), *Amorphophallus bulbifer* (HB) was resistant materials (R) (Wu et al. 2018). For plant pathogens, recognition of host plant via root exudates is the first step of successful invasion, but different plant species vary in their root exudate quantity and quality, so the effects on plant pathogens are also different. At present, there are many reports about the influence of plant root exudates on soil borne disease pathogens (Han et al. 2006; Huang et al. 2007) showed that after inoculation with *F. oxysporum*, the plant incidence rate of cucumber (*Cucumis sativus*) resistant varieties treated with root exudates was only 24.0%, while the plant incidence rate of susceptible varieties treated with root exudates was 41.0%, similar to the control. Ju et al (2022) analyzed the influence of cotton root exudates on the growth of fusarium wilt colony, the formation and germination of chlamydospores, and found that the root exudates of resistant varieties can inhibit the formation of chlamydospores of fusarium wilt, while the root exudates of susceptible varieties can stimulate the formation of chlamydospores. Zhou et al (2011) found that the type and content of root exudates of eggplant disease resistant (susceptible) varieties directly affect the growth of *Verticillium dahliae.*

There were significant differences in the effects of root exudates on the activity of pathogen among different varieties. Therefore, deciphering the metabolites in root exudates is important to understanding plant–pathogen interactions belowground. In this study, we systematically investigate the metabolites of root exudates from a soft rot resistant and a soft rot susceptible konjac, aiming to investigate the correlation between root exudates and disease resistance. The results provide an insight into the plant defense soft rot strategies mediated by root exudates.

2. Material and methods

2.1 Materials

The susceptibility konjac species "*Amorphophallus konjac* K.Koch" (HK), the resistance species "*Amorphophallus bulbifer*" (HB) were obtained from the Institute of Konjac, Enshi Academy of Agricultural Sciences, Enshi, P. R. China.

2.2 Root Exudate Collection

The experiments were carried out in Agricultural High Technology Zone of Enshi Tujia and Miao Autonomous Prefecture, Hubei province, China (30.3172°N, 109.4772°E, 421.5 m a.s.l). This region has a typical mid-subtropical monsoon type mountain humid climate with an average annual precipitation of 1400–1500 mm and an average temperature of 16.7°C. On April 10, about 50g of konjac corms (HK and HB) cultured in sterilized potting soil (20 cm × 20 cm) were used for the greenhouse experiment. Root exudates were collected when the konjac plants had reached a vigorous growth stage. On August 20, konjac was carefully dug up, the soil attached to the root surface was rinsed with tap water, and the roots were washed three times with distilled water. Three seedlings were put in a conical flask (500 ml), and the roots immersed in 300 ml of distilled water. After incubation under aeration conditions for 6 hours, the culture solution was freeze-dried, weighed, and transferred to a test tube with 10 ml of precooled methanol, and stored at -80°C. The weight of lyophilized exudates was 43.70 ± 2.93 mg in each treatment. Each treatment was repeated six times.

2.3 Analysis of Root Exudates

An UHPLC-Q Exactive HF-X system was used to separate and analyze the metabolites of root exudates. 2μL of sample was separated by HSS T3 (100 mm × 2.1 mm i.d. × 1.8 μm; Waters, Milford, USA) column entered into mass spectrometry detection. Mobile phase A was 95% water and 5% acetonitrile (containing 0.1% formic acid), and mobile phase B was 47.5% acetonitrile, 47.5% isopropanol and 5% water (containing 0.1% formic acid). The solvent gradient changed is referred to Shen et al (2023). The sample injection volume was 2 μL and the flow rate was 0.4 mL/min. The column temperature was maintained at 40 ℃. All these samples were stored at 4 ℃ during the period of analysis.

The mass spectrometric data was collected using a Thermo UHPLC -Q Exactive HF-X Mass Spectrometer equipped with an electrospray ionization (ESI) source operating in either positive or negative ion mode. The optimal conditions were same to the Shen et al (2023). Full MS resolution was 60000, and MS/MS resolution was 7500. The Data Dependent Acquisition (DDA) mode was used to data acquisition. The detection was carried out in range of 70-1050 m/z. A quality control (QC) sample was randomly inserted into every 5–15 analysis samples, in order to ensure the reliability and stability of the detection results. QC samples were prepared by mixing the extracts of all samples in equal volumes. The injection and detection methods of the QC samples are consistent with those of the normal samples.

2.4 UHPLC -Q Exactive HF-X Data Processing and Analysis

After the mass spectrometry detection was completed, the raw data of LC/MS was preprocessed using Progenesis QI (Waters Corporation, Milford, USA) software, and the three-dimensional data matrix in CSV format was exported. The three-dimensional matrix encompasses sample information, metabolite name and mass spectral response intensity. Internal standard peaks and known false positive signals (including noise, column bleed, and derivatized reagent peaks) were systematically eliminated from the data matrix through de-redundancy and peak pooling processes. Metabolites were scrutinized and authenticated utilizing the HMDB (http://www.hmdb.ca/), Metlin (https://metlin.scripps.edu/), and Majorbio Database.

The data after the database search was uploaded to the Majorbio cloud platform (https://cloud.majorbio.com) for comprehensive analysis. Metabolic features detected in at least 80% of any set of samples were meticulously retained following stringent filtration criteria. Minimum metabolite values were imputed for specific samples in which the metabolite levels fell below the lower limit of quantitation. Each metabolic feature underwent normalization by sum to mitigate errors stemming from sample preparation intricacies and instrument instability. Variables exhibiting a relative standard deviation (RSD) exceeding 30% of quality control (QC) samples were expunged, followed by log10 transformation to perform the definitive data matrix for subsequent analytical procedures.

2.5 Differential metabolites analysis

Perform variance analysis on the matrix file after data preprocessing (Liao et al. 2024). The R package ropls (Version 1.6.2) conducted principal component analysis (PCA) and orthogonal least partial squares discriminant analysis (OPLS-DA), and utilized 7-cycle interactive validation to assess model stability. Additionally, student's t-test and fold difference analysis were executed. Significantly different metabolites were selected based on Variable importance in the projection (VIP) obtained from the OPLS-DA model and the p-value of student’s t test, and the metabolites with VIP > 1, $p < 0.05$ were considered significantly different.

Differential metabolites between two groups were summarized and mapped to their biochemical pathways through metabolic enrichment and pathway analysis using database search (KEGG, http://www.genome.jp/kegg/). These metabolites can be categorized based on the pathways they are involved in or the functions they perform. Enrichment analysis was used to determine whether a group of metabolites appears in a specific function node or not. The principle was that the annotation analysis of a single metabolite develops into an annotation analysis of a group of metabolites.scipy.stats (Python packages) (https://docs.scipy.org/doc/scipy/) was employed for identifying statistically significantly enriched pathway using Fisher’s exact test.

3. Results

3.1 Metabolite Quantitative Analysis Between Resistant and Susceptible Konjac Species

The robustness of the LC-MS/MS-based metabolomic methodology was evaluated through a comprehensive analysis of the total ion chromatograms from Quality Control (QC) samples, which exhibited a consistent retention time and no significant peak drift. There were 14252 and 20756 ions identified in each sample profile in ESI + and ESI- mode, respectively. After removing low-quality ions [relative standard deviation (RSD) > 30%], 12442 and 16740 ions in each sample were identified in ESI + or ESI − mode, respectively. A total of 1122 metabolites were detected under positive and negative ion mode, of which 706 named metabolites in positive and negative ion mode were finally identified and confirmed based on the human metabolome database (HMDB). The dataset's reproducibility was ensured by QC sample measurement throughout the experimental process. Principal Component Analysis (PCA) was employed to differentiate between QC and test samples, as evidenced by two-dimensional PCA score plots (Figure S1). The results showed that QC samples were clustered closely to each other and were separated from the tested samples, confirming the stability and reproducibility of the LC-MS/MS analysis. To more specifically model differences between the species of konjac and to select features of interest in the data, partial least squares-discriminant analysis (PLS-DA) was applied (Figure.1). The first two principal components of the PLS-DA score plot was responsible for ESI (-) 80.9% (76.3% for component 1 and 4.6% for component 2) (Figure.1a) and ESI (+) 86.5% (68.1% for component 1 and 18.4% for component 2) (Figure.1b) of the overall variance of the metabolite profiles, showing a clear separation of the two konjac species. The metabolic profile disparities between konjac species were confirmed. At the same time, the ellipse representing the 95% confidence interval was notably larger for the HB, suggesting

a broader metabolic variability within this group. The validation of the PLS-DA models presented a high interpretation rate (R2Y) and prediction degree (Q2 > 0.5), indicating a higher reliability of these models.

3.2 Screening and Classification of the Differential Metabolites

A total of 364 potential metabolites with significant differential amounts among the two konjac species were screened by statistical analysis, and the overall profile of these differential metabolites in comparison of the two konjac species is shown in the volcano plots (Fig. 2, Table 1). Fold-change analysis was utilized to assess the regulation of these compounds, the abundances of compounds were exceed 1.5-fold and $P<0.05$ was regarded as significant difference. Log-fold changes > 1 and ≤ 1 were conceived as upregulation and downregulation, respectively, while changes between − 1 and 1 were not considered to represent changes in regulation. In HK/HB, there are 12 upregulation metabolites, 14 downregulated metabolites and 1065 unchanged metabolites. As can be seen from Fig. <link rid="fig3">3</link>, 1,3-dideacetyl-7-deacetoxy-7-oxokhivori, DG(18:0/20:4(8Z,11Z,14Z,17Z)/0:0), 3-Fucosyllactose, 35-aminobacteriohopane-30,31,32,33,34-pentol, lysoPC(18:2(9Z,12Z)), lansioside A and 7,8-Dihydrovomifoliol 9-[rhamnosyl-(1->6)-glucoside] only showed in HB. 6-{4-[3-(4,5-dihydroxy-7-methoxy-2,2-dimethyl-3,4-dihydro-2H-1-benzopyran-6-yl)-3-oxopropyl] phenoxy}-3,4,5-trihydroxyoxane-2-carboxylic acid, guanosine diphosphate adenosine, solacauline and Uridine diphosphate-N-acetylglucosamine only showed in HK. These metabolites are mainly classified as organic oxygen compounds and lipids and lipid-like molecules in HB, Phenylpropanoids and polyketides, Nucleosides, nucleotides, and analogues, Lipids and lipid-like molecules in HK (Table 2).

Table 1
Discriminant metabolites in the positive and negative ion modes in root exudates under different konjac species.

Metabolite	Metab ID	Regulate	Formula	HMDB Superclass	FC(HK/HB)
Uridine diphosphate-N-acetylglucosamine	metab_33687	up	$C_{17}H_{27}N_3O_{17}P_2$	Nucleosides, nucleotides, and analogues	2.0726
Cytidine diphosphate (CDP)	metab_34400	up	$C_9H_15N_3O_11P_2$	-	2.1436
Uridine diphosphate (UDP)	metab_17892	up	$C_9H_{14}N_2O_{12}P_2$	-	2.1198
CL(18:2(9Z,12Z)/18:2(9Z,12Z)/18:2(9Z,12Z)/18:3(9Z,12Z,15Z))	metab_1790	up	$C_{81}H_{140}O_{17}P_2$	Lipids and lipid-like molecules	2.3205
ADP	metab_14698	up	$C_{10}H_{15}N_5O_{10}P_2$	Nucleosides, nucleotides, and analogues	1.9957
Guanosine diphosphate adenosine	metab_18381	up	$C_{20}H_{26}N_{10}O_{14}P_2$	Nucleosides, nucleotides, and analogues	1.9025
5'-CMP	metab_3951	up	$C_9H_{14}N_3O_8P$	Nucleosides, nucleotides, and analogues	1.6092
Aconitic acid	metab_35000	up	$C_6H_6O_6$	Organic acids and derivatives	1.5375
N-Ribosylhistidine	metab_9697	up	$C_{11}H_{17}N_3O_6$	Organic acids and derivatives	1.5901
Sulindac sulfone	metab_29210	up	$C_{20}H_{17}FO_4S$	Benzenoids	1.541
DIURON	metab_21735	up	$C_9H_{10}C_{l2}N_2O$	-	1.5392
2-{9-hydroxy-2-oxo-2H,8H,9H-furo [2,3-h]chromen-8-yl}propan-2-yl (2E)-3-(2,4-dihydroxyphenyl)prop-2-enoate	metab_5750	up	$C_{23}H_{20}O_8$	Phenylpropanoids and polyketides	1.5361
Buddleoflavonoloside	metab_1714	down	$C_{28}H_{32}O_{14}$	-	0.5606
35-aminobacteriohopane-30,31,32,33,34-pentol	metab_8243	down	$C_{35}H_{63}NO_5$	-	0.4706
Physalolactone	metab_4325	down	$C_{28}H_{39}ClO_8$	Nucleosides, nucleotides, and analogues	0.6039
Hesperetin 7-neohesperidoside	metab_19995	down	$C_{28}H_{34}O_{15}$	Phenylpropanoids and polyketides	0.612
6-[(1Z)-2-hydroxy-3-oxobut-1-en-1-yl]-7-methoxy-2H-chromen-2-one	metab_11925	down	$C_{14}H_{12}O_5$	Phenylpropanoids and polyketides	0.5968
1,3-dideacetyl-7-deacetoxy-7-oxokhivorin	metab_5737	down	$C_{26}H_{34}O_7$	-	0.5459
Equol	metab_21793	down	$C_{15}H_{14}O_3$	Phenylpropanoids and polyketides	0.4855
9,10-dihydroxy-8,8-dimethyl-2H,8H, 9H,10H-pyrano[2,3-h]chromen-2-one	metab_12093	down	$C_{14}H_{14}O_5$	Phenylpropanoids and polyketides	0.6213
Uric acid	metab_33896	down	$C_5H_4N_4O_3$	Organoheterocyclic compounds	0.6049
Armillarivin	metab_22624	down	$C_{23}H_{28}O_5$	Lipids and lipid-like molecules	0.579
PE(P-16:0/16:1(9Z))	metab_24360	down	$C_{37}H_{72}NO_7P$	Lipids and lipid-like molecules	0.5669
3-Fucosyllactose	metab_3906	down	$C_{18}H_{32}O_{15}$	Organic oxygen compounds	0.6143
N,N'-bis(3-aminopropyl)butane-1,4-diamine	metab_14205	down	$C_{10}H_{26}N_4$	Organic nitrogen compounds	0.6417
Neryl rhamnosyl-glucoside	metab_20661	down	$C_{22}H_{38}O_{10}$	Lipids and lipid-like molecules	0.6533
Jasmonic acid	metab_33071	down	$C_{12}H_{18}O_3$	Lipids and lipid-like molecules	0.6893

Table 2
Specific metabolites in root exudates under different konjac species.

Different konjac species	Metabolite	Formula	HMDB Superclass
HB	3-Fucosyllactose	$C_{18}H_{32}O_{15}$	Organic oxygen compounds
	1,3-dideacety-7-deacetox-7-oxokhivori	$C_{26}H_{34}O_7$	-
	DG(18:0/20:4(8Z,11Z,14Z,17Z)/0:0)	$C_41H_{72}O_5$	Lipids and lipid-like molecules
	35-aminobacteriohopane-30,31,32,33,34-pentol	$C_{35}H_{63}NO_5$	-
	LysoPC(18:2(9Z,12Z))	$C_{26}H_{50}NO_7P$	Lipids and lipid-like molecules
	Lansioside A	$C_{38}H_{61}NO_8$	Lipids and lipid-like molecules
	7,8-Dihydrovomifoliol 9-[rhamnosyl-(1->6)-glucoside]	$C_{25}H_{42}O_{12}$	Lipids and lipid-like molecules
HK	6-{4-[3-(4,5-dihydroxy-7-methoxy-2,2-dimethyl-3,4-dihydro-2H-1-benzopyran-6-yl)-3-oxopropyl]phenoxy}-3,4,5-trihydroxyoxane-2-carboxylic acid	$C_{27}H_{32}O_{12}$	Phenylpropanoids and polyketides
	Guanosine diphosphate adenosine	$C_{20}H_{26}N_{10}O_{14}P_2$	Nucleosides, nucleotides, and analogues
	Solacauline	$C_{43}H_{69}NO_{14}$	Lipids and lipid-like molecules
	Uridine diphosphate-N-acetylglucosamine	$C_{17}H_{27}N_3O_{17}P_2$	Nucleosides, nucleotides, and analogues

The HMDB 4.0 database was compared to obtain the classification information of metabolites and plotted statistical mapping. The differential metabolites were assigned to various chemical categories, including lipids and lipid-like molecules (41.91%), organic acids and derivatives (15.07%), phenylpropanoids and polyketides (13.97%), organic oxygen compounds (9.93%), organoheterocyclic compounds (6.62%), benzenoids (5.15%), nucleosides, nucleotides, and analogues (4.41%), organic nitrogen compounds (2.94%) (Fig. 4). As shown in Table 1, the unique upregulated metabolites belong to organic acids/derivatives/benzenoids, which the unique downregulated metabolites belong to organoheterocyclic compounds/organic oxygen compounds/organic nitrogen compounds.

3.3 Metabolic Pathway Analysis Based on the KEGG Database

The differential metabolites between resistant and susceptible konjac specie were involved in a total of 79 pathways or metabolisms, including Carbohydrate metabolism, Energy metabolism, Amino acid metabolism, Nucleotide metabolism, Metabolism of other amino acids, Metabolism of cofactors and vitamins, Metabolism of terpenoids and polyketides, Biosynthesis of other secondary metabolites, Lipid metabolism, Global and overview maps, and the 13 most enriched pathway terms are shown in the KEGG enrichment bubble diagrams, and Citrate cycle, Arginine biosynthesis, Purine metabolism, Arginine and proline metabolism were significantly impacted by HB (Fig. 5).

4. Discussion

4.1 Differential Metabolite Analysis in Root Exudates

The activity of root exudates of different resistant crop varieties to pathogens was related to their chemical components. Therefore, the analysis of chemical components in root exudates is of great significance in understanding the interactions between different disease-resistant varieties and pathogens. GC-MS and LC-MS may help to generate a spatially explicit metabolome of the root and its exudates at a scale that is relevant for the rhizosphere community (Van Dam et al. 2016). The non-targeted metabolome analysis based on an UHPLC-Q Exactive HF-X system revealed that the root exudates of konjac a wide variety of compounds (Fig. 4), including Lipids and lipid-like molecules (41.91%), Organic acids and derivatives (15.07%), Phenylpropanoids and polyketides (13.97%), Organic oxygen compounds (9.93%), Organoheterocyclic compounds (6.62%), Benzenoids (5.15%), Nucleosides, nucleotides, and analogues (4.41%), Organic nitrogen compounds (2.94%). The results were consistent with those of other reported crop root exudates (Lucini et al. 2019).

OPLS-DA analysis of the metabolic profile of root exudates indicated that root exudate components were influenced by plant genotype. Further analysis of the differential metabolites showed that there were 7 unique metabolites in HB, belonging to organic oxygen compounds and lipids and lipid-like molecules, and 4 unique metabolites in HK, belonging to phenylpropanoids and polyketides, nucleosides, nucleotides, and analogues, lipids and lipid-like molecules (Table 2). The fold change is 0.6143 in HK/HB (Table 1) for 3-Fucosyllactose.We know that the 3-Fucosyllactose play an important role in plant disease resistance. Fucoidan is a component of seaweed polysaccharide. Seaweed polysaccharide as plant growth stimulators, which regulates stress signals, and supports plant biochemical processes (Gurusarava et al. 2017; Circuncisão et al. 2018). For plant pathogens, recognition of host plant via

root exudates is the first step of successful invasion, the use of seaweed polysaccharide can affect the composition of rhizosphere soil microbial community enhance biotic stress and abiotic stress tolerance in plants, thereby improving crop disease resistance (Sarkar et al. 2018; Karthik et al. 2020). This may be one of the reasons why HB has higher disease resistance than HK.

Root exudates are the most important secondary metabolites of plant roots, which can carry the material exchange and information transfer between plants and soil. Exudation is key factors of micro-ecological characteristics of different rhizosphere of plants, which can exert beneficial or harmful effects on soil microorganisms (including pathogens) and plants, and are closely related to plant disease resistance. Different plant species vary in their root exudate quantity and quality, which results in different resistance of plants to pathogens (Yang et al. 2014). Buddleoflavonoloside, 6-[(1Z)-2-hydroxy-3-oxobut-1-en-1-yl]-7-methoxy-2H-chromen-2-one, 9,10-dihydroxy-8,8-dimethyl-2H,8H,9H,10H-pyrano[2,3-h]chromen-2-one and Equol belong to flavonoi, which are downregulated in HK/HB metabolites (Table 1). The flavonoid had been shown to have significant inhibitory effects on some plant pathogens (Li et al. 2022). It is reported that the resistance of alfalfa to fusarium wilt is closely related to the isoflavone pathway (Gill et al. 2018). In cucumber, many metabolites related to flavonoid biosynthesis are up-regulated after infection with Sphaerotheca fuliginea, suggesting that increasing the content of flavonoid may play an important role in resistance formation (Zhang et al. 2021). For example, flavonoids exuded through plant roots are known to recruit specific arbuscular mycorrhizal fungi (Steinkellner et al. 2007); colonization of maize roots, by growth promoting and systemic resistance inducing Pseudomonas putida, is driven by exudation of the benzoxazinoid DIMBOA (Neal et al. 2012). The accumulations of flavonoids in HK were 0.5606,0.5968,0.6213 and 0.4855 times of HB. The differential accumulation of flavonoids in konjac resulted in the strong disease resistance of HB.

4.2 Analysis of different metabolic pathways

Plant hormone signal transduction and flavonoid biosynthesis are involved in Plant disease resistance biosynthesis, while Jasmonic acid (JA), which is involved in plant hormone signal transduction metabolism, and Hesperetin 7-neohesperidoside, which is involved in flavonoid biosynthesis, is down-regulated in HK/HB (Table 1). Plant hormones crosstalk mediate complex signal transduction networks, involve in different defense strategies to pathogens (Li et al.2019). JA is an important stress-associated phytohormone that can promote various defense interactions, regulate stomatal openness, synthesis of antimicrobial substances, or plant cell reprogramming (Omar et al. 2023). For example, Jasmonic acid contributes to rice resistance against Magnaporthe oryzae (Ma et al. 2022) For example, MeJA induces the PR-1b and osmotin (PR-5) mRNA accumulation in tobacco, also cause efficient reduction of disease development by *Alternaria brassicicola, Botrytis cinerea*, and *Plectosphaerella cucumerina* in Arabidopsis, and delays symptom development by the crown rot pathogen *Fusarium pseudograminearum* in wheat (Desmond et al. 2005; Wasternack 2007). Jasmonic acid contributes to rice resistance against *Magnaporthe oryzae Flavanones* belong to a unique class of polyphenols containing three main aglycones: hesperetin, eriodictyol and naringenin (Manach et al. 2003). Flavonoids are an essential factor in plant interactions with the environment, often serving as the first line of defense against pathogen attacks (Wang et al. 2011), so that we conjectured that jasmonic acid contributes to konjac resistance against soft rot. Neohesperidin (hesperetin 7-O-neohesperidoside), a well-known flavanone glycoside widely found in citrus fruits, exhibits a variety of biological activities, with potential applications ranging from food ingredients to therapeutics (Akhter et al. 2022). The levels of flavonoids involved in the defense mechanism of citrus aurantium fruits against *Peniillium digitatum* (Arcas et al. 2000). The results showed that HB is more resistant to soft rot than HK.

5. Conclusion

Our results indicated that the root exudates not only provide a pre-infection prevention strategy by exuding antimicrobial substances, but also increase konjac disease resistance by eliciting plant defense responses. This study provides a new way to prevent and control soft rot disease of konjac by using secondary metabolism of plants.

Declarations

Acknowledgements

The work was financially supported by grants from the Nature Science Foundation of China [Grant Number 32072558]. Hubei Agricultural Science and technology Innovation Center innovation team project [Grant Number 2021-620-000-001-01]

Disclosure statement

No potential conflict of interest was reported by the author(s).

Notes on contributors

Jinping Wu conceived and designed the experiments. Jie Zhou, Zhao qinghua, Yang Chaozhu and Chuangdong Qi performed the experiments. Jinping Wu and Fengling Guo wrote and revised the manuscript. All authors approved the final version of the manuscript.

Data availability statement

The original contributions presented in this study are included in the article/supplementary material, further inquiries can be directed to the corresponding author.

References

1. Akhter S, Arman MSI, Tayab MA, Islam MN, Xiao J (2022) Recent advances in the biosynthesis, bioavailability, toxicology, pharmacology, and controlled release of citrus neohesperidin. Crit Rev Food Sci Nutr 23:1–20. 10.1080/10408398.2022.2149466
2. Arcas MC, Botía JM, Ortuño AM, del Rio JA (2000) UV irradiation alters the levels of flavonoids involved in the defence mechanism of Citrus aurantium fruits against Peniillium digitatum. Eur J Plant Pathol 106:617–622
3. Circuncisão AR, Catarino MD, Cardoso SM, Silva AM (2018) Minerals from macroalgae origin: health benefits and risks for consumers. Mar Drugs 16:400. https://doi.org/10.3390/md16110400
4. Desmond OJ, Edgar CI, Manners JM, Maclean DJ, Schenk PM, Kazan K (2005) Methyl jasmonate induced gene expression in wheat delays symptom development by the crown rot pathogen *Fusarium pseudograminearum*. Physiol Mol Plant P 67(3–5):171–179
5. Gill US, Uppalapati SR, Gallego-Giraldo L (2018) Metabolic flux towards the (iso) flavonoid pathway in lignin modified alfalfa lines induces resistance against *Fusarium oxysporum f. sp. medicaginis*. Plant Cell Environ 1:1997–2007
6. Gu HH, Wang ZX, Jiang X (2018) Soft rot of Amorphophallus and its control research progress. Agric J 8:15–19
7. Gurusarava P, Vinoth S, Prem Kumar G, Pandiselvi (2017) Seaweed extract promotes high-frequency in vitro regeneration of *Solanum surattense Burm. f.* a valuable medicinal plant. Res J Med Plants 11:134–141. https://doi.org/10.3923/rjmp.2017.134.141
8. Han X, Wu F-Z, Pan K (2006) Review on the relation between the root exudates and soil-spread disease. Chin Agric Sci Bull 22(3):316–318
9. Huang BL, Xu YD, Wu Y (2007) Effects of root exudates from cucumber and squash on Fusarium wilt occurrence. Chin J Appl Ecol 8(3):559–563
10. Jiang X, Wang ZX, Yang FQ, Chen ZZ, Yang SM, Yan ZS, Qin YG (2021) Effects of different pesticide treatments on soft rot control and yield of konjac. IOP Conf Ser: Earth Environ Sci 687:012049. 10.1088/1755 – 1315/687/1/012049
11. Ju FY, Li Y, Zhang XH, Yu K, Huo YY, Zhu JJ, Wang YH, Zhou ZG, Ali S, Tang QX, Chen BL (2022) Effects of potassium application on soil ecological resistance to Verticillium wilt of cotton (*Gossypium hirsutum* L). Arch Agron Soil Sci 68(4):488–502. https://doi.org/10.1080/03650340.2020.1841173
12. Karthik T, Sarkar G, Babu S, Amalraj LD, Jayasri MA (2020) Preparation and evaluation of liquid fertilizer from Turbinaria ornata and Ulva reticulata. Biocatal Agric Biotechnol 28:101712. https://doi.org/10.1016/j.bcab.2020.101712
13. Li DY, Yue LX, Wang SG (2022) Quercitrin restrains the growth and invasion of lung adenocarcinoma cells by regulating gap junction protein beta 2. Bioengineered 13(3):6126–6135
14. Li N, Han X, Feng D, Yuan D, Huang LJ (2019) Signaling crosstalk between salicylic acid and ethylene/jasmonate in plant defense: Do we understand what they are whispering? Int J Mol Sci 20(3):671
15. Liao W, Guo R, Qian K, Shi W, Whelan J, Shou H (2024) The acyl-acyl carrier protein thioesterases GmFATA1 and GmFATA2 are essential for fatty acid accumulation and growth in soybean. Plant J 15. 10.1111/tpj.16638
16. Liu E, Yang C, Liu J (2019) Comparative analysis of complete chloroplast genome sequences of four major Amorphophallus species. Sci Rep 9:809. https://doi.org/10.1038/s41598-018-37456-z
17. Lucini L, Colla G, Miras Moreno MB, Bernardo L, Cardarelli M, Terzi V, Bonini P, Rouphael Y (2019) Inoculation of Rhizoglomus irregulare or Trichoderma atroviride differentially modulates metabolite profiling of wheat root exudates. Phytochem 57:158–167. 10.1016/j
18. Manach C, Morand C, Gil-Izquierdo A, Bouteloup-Demange C, and Rémésy C (2003) Bioavailability in humans of the flavanones hesperidin and narirutin after the ingestion of two doses of orange juice. Eur J Clin Nutr 57:235–242. 10.1038/sj.ejcn.1601547
19. Ma J, Morel JB, Riemann M, Nick P (2022) Jasmonic acid contributes to rice resistance against Magnaporthe oryzae. BMC Plant Biol 22(1):601. 10.1186/s12870-022-03948-4
20. Van Dam NM, Bouwmeester HJ (2016) Metabolomics in the Rhizosphere: Tapping into Belowground Chemical Communication.Trends Plant Sci. 256–265. 10.1016/j.tplants
21. Omar AH, Nabil IE, Ali MK, Neveen E, Ramadan AA, Ghada AM, Mona FD, Walaa EH, Abdelaziz M, Dina H, Suleyman IA, Marek Z, Marian B (2023) Jasmonic acid regulates plant development and orchestrates stress response during tough times. Environ Exp Bot 208:105260. https://doi.org/10.1016/j.envexpbot
22. Sarkar G, Jatar N, Goswami P, Cyriac R, Suthindhiran K, Jayasri MA (2018) Combination of different marine algal extracts as biostimulant and biofungicide. J Plant Nutr 41:1163–1171. https://doi.org/10.1080/01904167.2018.1434201
23. Wang Y, Chen S, Yu O (2011) Metabolic engineering of flavonoids in plants and microorganisms. Appl Microbiol Biotechnol 91(4):949–956. 10.1007/s00253-011-3449-2
24. Wu X, Yang M, Liu JN, Chen ZB, Wang DK, Zhao JR, Zhong Y, Wu DX, Yu L (2018) Identification and Evaluation of Resistance of *Amorphophallus* spp. to *Erwinia carotovora subsp. carotovora*. Subtropical plant sci 47(2):176–180
25. Yang RX, Gao ZG, Liu X, Yao Y, Cheng Y (2014) Root exudates from muskmelon (*Cucumis melo* L.) induce autotoxicity and promote growth of *Fusarium oxysporum f. sp.melonis*. Allelopathy J 33(2):175–188
26. Zhang Z, Li J, Zhang Z (2021) Tomato endophytic bacteria composition and mechanism of suppressiveness of wilt disease (*Fusarium oxysporum*). Front Microbiol 12:731764
27. Zhou BL, Chen ZX, Du L (2011) Allelopathy of the root exudates from different resistant eggplants to Verticillium wilt (*Verticillium dahliae Kleb*). Acta Ecol Sin 31(14):3964–3972

28. Zhou BL, Liu a, Ye XL, Lu B (2011) Effect of grafting eggplant on root exudates and disease resistance under Verticillium dahliae stress. Acta Ecol Sin 31(3):0749–0759

Figures

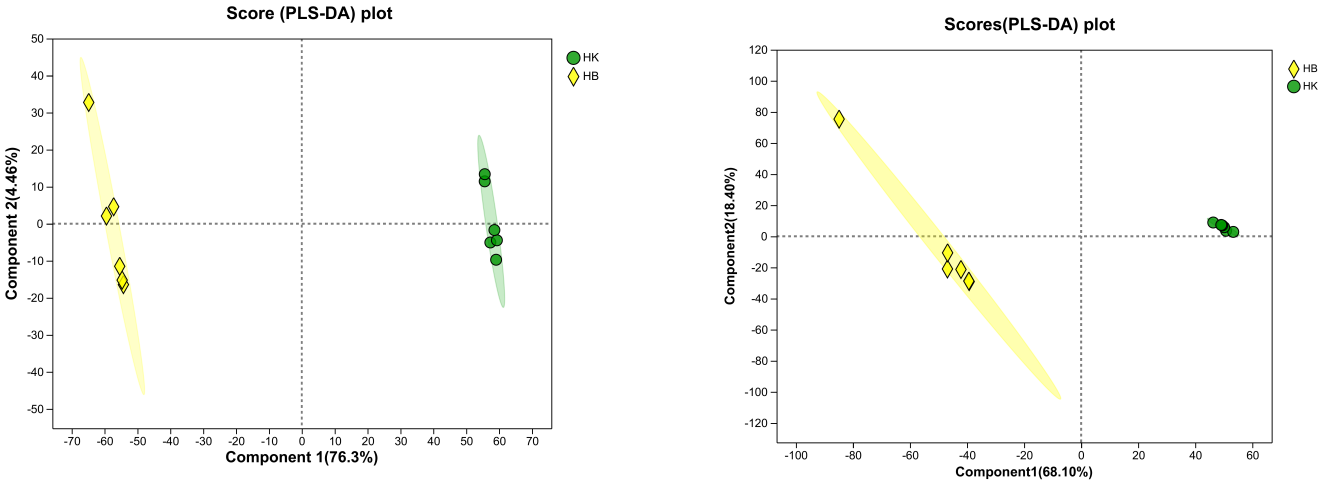

Figure 1

Partial least squares discriminant analysis of untargeted metabolomics data root exudates of different konjac species. Ellipses represent the 95% confidence interval. a) liquid chromatography-mass spectrometry ESI (+) b) liquid chromatography-mass spectometry ESI (-). Yellow rhombus, HB; green dot, HK; Abbreviation: HK, *Amorphophallus konjac K.Koch*; HB, *Amorphophallus bulbifer*.

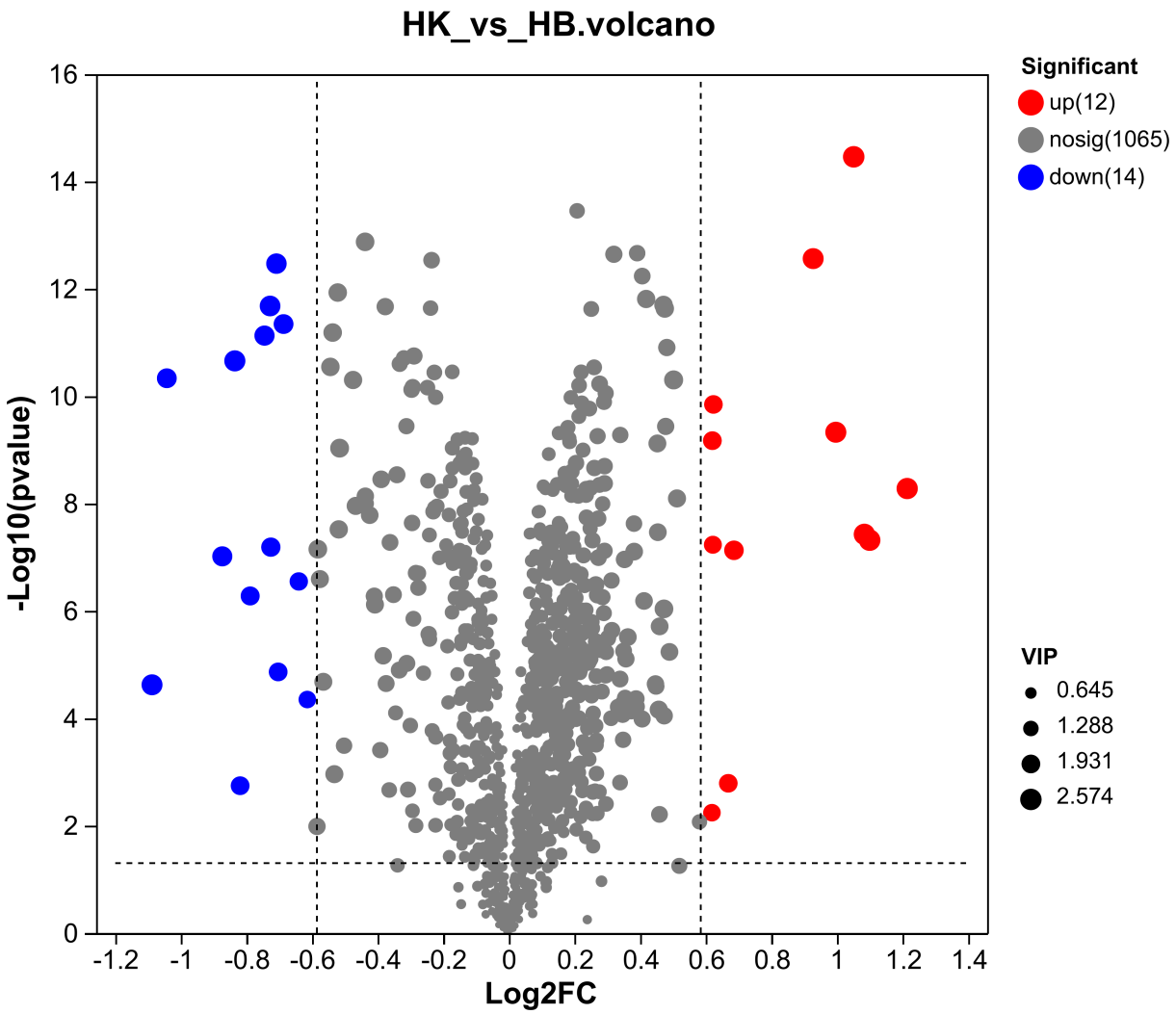

Figure 2

The volcanic plots of differential metabolites in pairwise comparison under different konjac species.

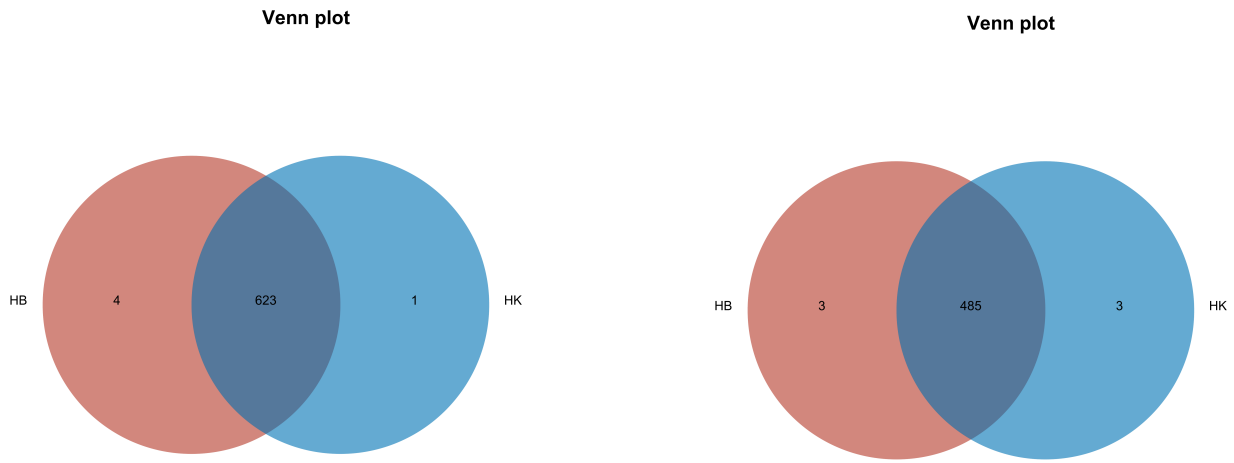

Figure 3

Venn diagram of differential accumulated metabolites in root under different konjac species. a) liquid chromatography-mass spectrometry ESI (+) b) liquid chromatography-mass spectometry ESI (-).

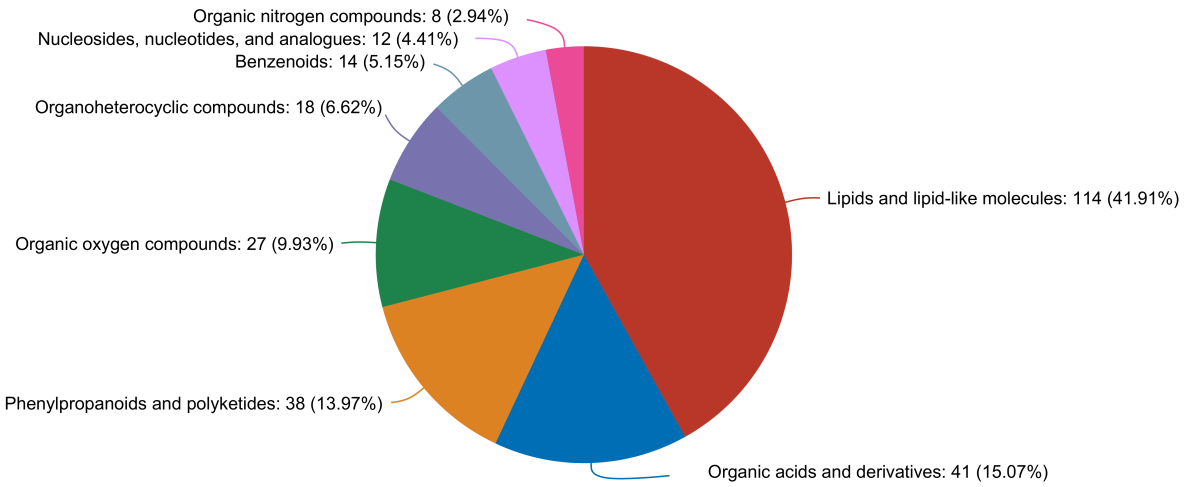

Figure 4

Classification and statistics of metabolites in root exudates under different konjac species.

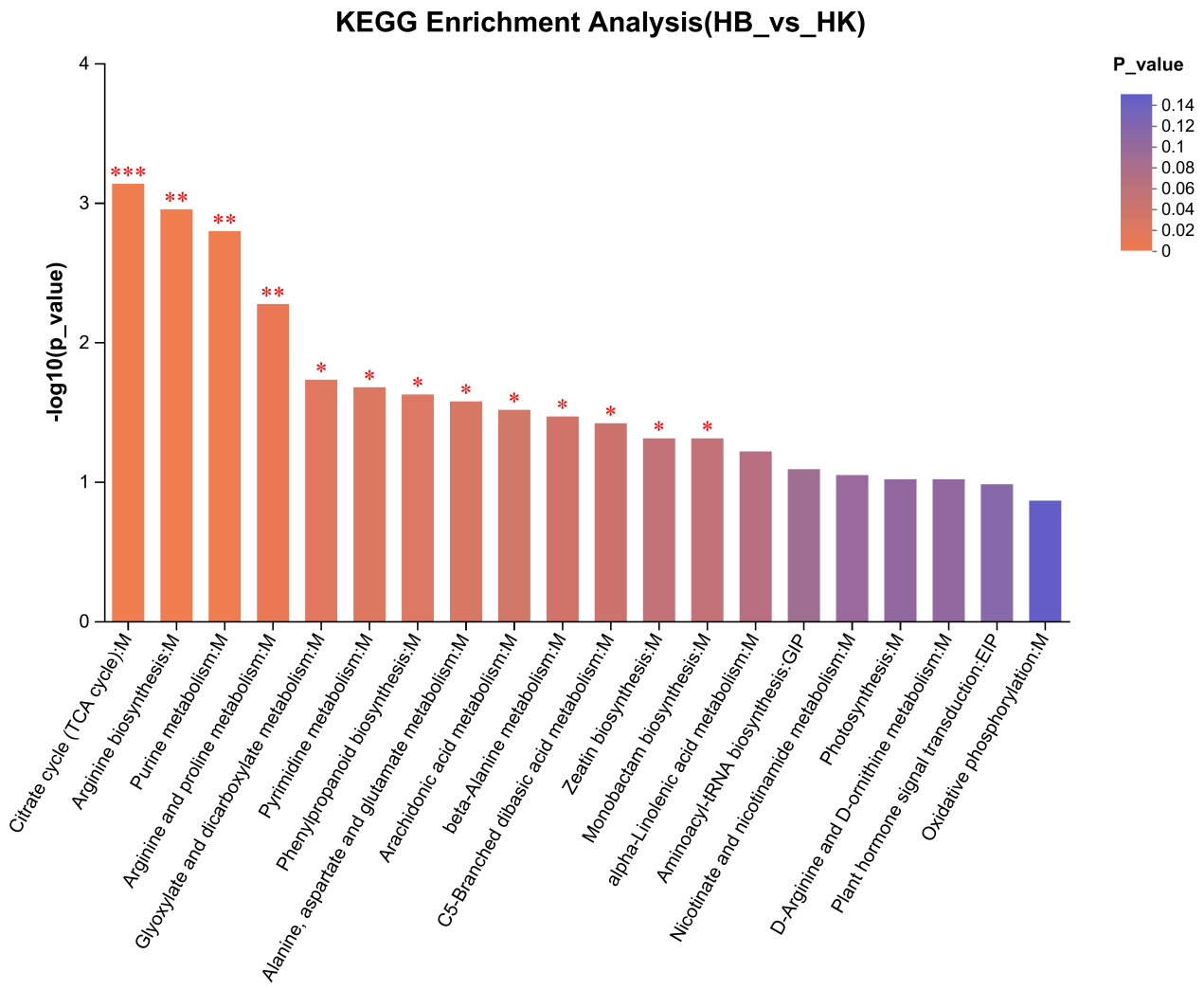

Figure 5

KEGG pathway analysis of Differentially accumulated metabolites in root exudates under different konjac species.

Supplementary Files

This is a list of supplementary files associated with this preprint. Click to download.

- FigS1a.png
- FigS1b.png